First Observation of a Wetting Phase Transition in Low-Angle Grain Boundaries

B. B. Straumal[a], B. S. Bokshtein[b], A. B. Straumal[b], and A. L. Petelin[b]

[a] *Institute of Solid State Physics, Russian Academy of Sciences, Chernogolovka, Moscow region, 142432 Russia*
e-mail: straumal@issp.ac.ru

[b] *State Technological University "Moscow State Institute of Steel and Alloys," Leninskiĭ pr. 4, Moscow, 119049 Russia*

Received August 11, 2008; in final form, September 9, 2008

The wetting phase transition at low-angle intercrystallite grain boundaries has been experimentally observed. In contrast to the high-angle grain boundaries with the misorientation angels $\theta > 15°$, the low-angle grain boundaries ($\theta < 15°$) are not continuous two-dimensional defects, but constitute a discrete wall (network) of lattice dislocations (edge and/or helical). The theory predicts that, depending on θ, either a continuous layer of the liquid phase or a wall (network) of microscopic liquid tubes on wetted dislocation nuclei is formed at completely wetted low-angle grain boundaries. It has been shown that the continuous liquid layers at low-angle grain boundaries in the Cu–Ag alloys appear at the temperature $T_{\text{wminL}} = 970°C$, which is 180°C higher than the onset temperature $T_{\text{wmin}} = 790°C$ and 50°C lower than the finish temperature of the wetting phase transition at high-angle grain boundaries, $T_{\text{wmax}} = 1020°C$.

If a two- or multicomponent polycrystalline solid solution is in equilibrium with a melt, the following two situations are possible.

(i) The melt incompletely wets the inner intercrystallite interfaces (grain boundaries) in the polycrystal. This means that the energy of the grain boundaries σ_{GB} is lower than the energy of two interfaces between the solid phase and melt, $2\sigma_{\text{SL}}$. In this case, the contact angle θ at the place of entering the grain boundary at the interface between the solid and liquid phases is given by the expression

$$\sigma_{\text{GB}} = 2\sigma_{\text{SL}}\cos(\theta/2). \qquad (1)$$

(ii) The melt completely wets the grain boundaries. In this case, $\sigma_{\text{GB}} \leq 2\sigma_{\text{SL}}$, the contact angle is zero, $\theta = 0$, and the melt layer should replace the grain boundary, separating crystallites from each other.

Cahn [1] and Ebner and Saam [2] demonstrated that the transition from incomplete wetting to complete wetting can occur with an increase in temperature and is a phase transition. This is possible if the temperature dependences $\sigma_{\text{GB}}(T)$ and $2\sigma_{\text{SL}}(T)$ intersect each other at a certain temperature T_{w} below the melting temperature T_{m} (see Fig. 1a). More recently, such transitions were observed in polycrystals [3, 4] and were investigated in more detail at single grain boundaries in specially grown bicrystals [4–6]. The temperature T_{w} depends on the energy of the grain boundary: T_{w} decreases with an increase in σ_{GB}. The wetting phase transition in the polycrystal starts at the temperature T_{wmin}, when the

grain boundaries with the maximum energy σ_{GBmax} become completely wetted (see Fig. 1b). The wetting phase transition in the polycrystal finishes at the temperature T_{wmax}, when the high-angle grain boundaries with the minimum energy σ_{GBmin} become completely wetted (see Fig. 1).

The above statements refer to the so-called high-angle grain boundaries, i.e., grain boundaries with a misorientation angle θ larger than approximately 15° (see Fig. 1b). Such boundaries constitute a continuous two-dimensional defect (layer) with a thickness of 0.5 nm between two neighboring grains at which the lattice planes of two crystallites forming the boundary break [7]. On the contrary, the boundaries with small misorientation angles (<15°) (low-angle grain boundaries) constitute an ensemble of one-dimensional defects, i.e., a wall or a network of lattice dislocations (edge and/or helical). In the spaces between the dislocations, the lattice planes of one of two crystallites forming the boundary smoothly transfers with a small bend to the lattice planes of the other crystallite. In the simplest case of the low-angle tilt boundary, its misorientation angle θ is determined by the distance b between the dislocations in the walls and their Burgers vector, and the energy of such a boundary is given by the Read–Shockley formula [8]

$$\sigma_{\text{GB}} = Gb\theta\ln(\alpha e/2\pi\theta)/[4\pi(1-\nu)], \qquad (2)$$

where G is the shear modulus, ν is Poisson's ratio, and α is the constant, which is close to unity for the fcc lat-
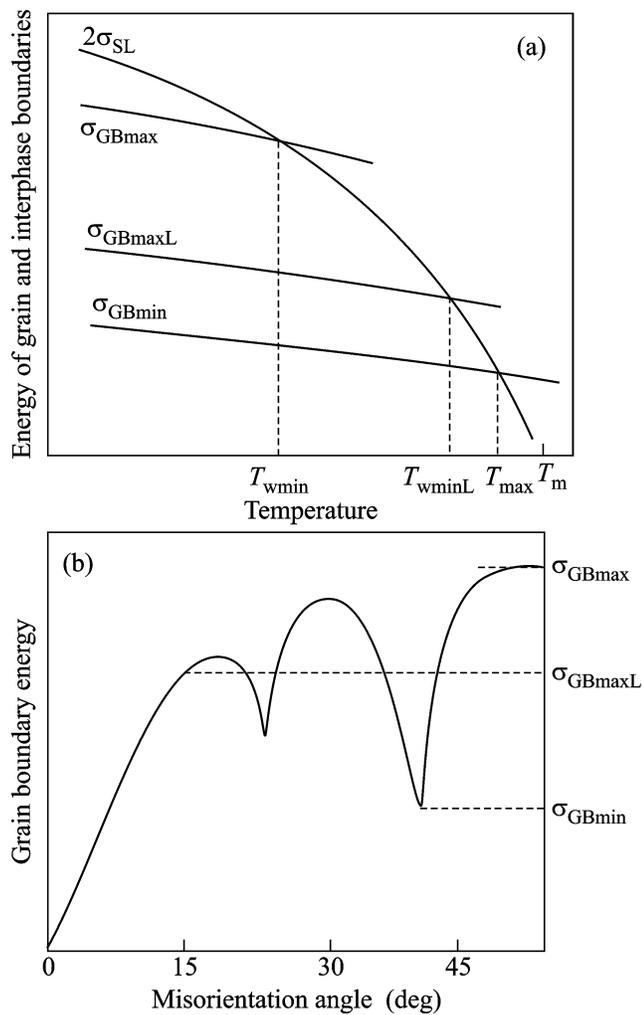
Fig. 1. (a) Schematic temperature dependences of the energies of the high-angle grain boundaries, $\sigma_{GB\,min}$ and $\sigma_{GB\,max}$, and low-angle grain boundaries, $\sigma_{GB\,maxL}$, and the energy of the interfaces between the solid and liquid phases, σ_{SL}. (b) Schematic misorientation-angle dependence of the energy of the grain boundaries. The minima correspond to special boundaries near the coincidence misorientation angles.

tice crystals, is close to four for germanium, and is between one and four for the bcc lattice crystals.

Rabkin and Snapiro [9] showed that two variants of the complete wetting of a low-angle grain boundary are possible. In the first case, the low-angle grain boundary, as well as the high-angle grain boundary, is replaced by the continuous layer of the liquid phase. In this case, the normal condition of the complete wetting, $\sigma_{GB} \leq 2\sigma_{SL}$, is satisfied and σ_{GB} is given by Eq. (2). In the second case, each dislocation of the low-angle grain boundary is replaced by a tube of the liquid phase (melt). The second case can occur only if the dislocations are sufficiently far from each other (i.e., the misorientation angle is sufficiently small); otherwise, tubes filled with the melt join and form a continuous layer as in the first

case. The equilibrium radius of the nucleus of the wetted dislocation R_F is given by the modified Frank formula [10] in which the outer-surface energy σ_S is changed to the energy σ_{SL} of the interface between the solid and liquid phases [9]

$$R_F = Gb^2/[8\pi^2(1-\nu)\sigma_{SL}]. \qquad (3)$$

According to estimates [8] for iron, $R_F = 0.44$ nm; i.e., the radius of the nucleus of the wetted dislocation is very small. Estimates in [9] also show that, if σ_{SL} is fixed, the liquid nuclei of dislocations can appear at a certain critical misorientation angle $\theta_{w1} = 0.19b/R_F$, and the coalescence of the liquid nuclei of dislocations begins at the misorientation angle $\theta_{w2} = 1.07b/R_F$. The quantitative estimates and indirect facts indicate that the transition from the incomplete wetting of low-angle grain boundaries to complete wetting can be observed [9, 11, 12]. However, dislocations with wetted nuclei (i.e., the first variant of the complete wetting of the low-angle grain boundary) have not yet been observed in direct experiments. Moreover, the formation of a continuous wetting layer at the low-angle grain boundary above a certain temperature T_w, which is often observed at boundaries with large misorientation angles [4], has not yet been observed. This work is devoted to the direct experimental observation of such a transformation.

For investigations by means of induction fusion in a vacuum, we melted copper alloys with 10, 8, and 5 wt % of silver (copper with a purity of 99.998 wt % and silver with a purity of 99.99 wt %). The ingots 10 mm in diameter were cut into 2-mm-thick disks; these disks were soldered into evacuated quartz ampoules. The ampoules with the samples were annealed for 2 h in a SUOL electric resistance furnace at temperatures ranging from 780 to 1050°C. The points corresponding to the annealing temperatures and alloy compositions are shown in Fig. 2. After annealing, the samples were hardened in water (ampoules were broken) and, then, were mechanically grinded and polished with a diamond paste with a cut of 1 μm. The resulting sections were studied using scanning electron microscopy and X-ray microanalysis by means of a Tescan Vega TS5130 MM microscope equipped with a LINK energy dispersive spectrometer (Oxford Instruments).

Figure 3a shows the microstructure of the copper alloy with 10 wt % Ag after annealing at a temperature of 800°C. It includes two structural components, dark and light. The dark structural component (matrix) is a solid solution based on copper with the silver concentration corresponding to the solidus line at the annealing temperature (i.e., approximately 8 wt % Ag). The light structural component locating at the boundaries and triple joints is formed after the hardening from the silver-rich alloy with the composition on the liquidus line. The grain boundaries completely wetted by the melt, which are completely (from one triple joint to another triple point) replaced by the melt layer, are

almost absent in the structure shown in Fig. 3a. The arrows mark one completely wetted boundary as an example in each of Figs. 3a and 3b. In Fig. 3a, the melt forms separated, although very flat, drops at most grain boundaries. The first grain boundaries completely wetted by the melt appear at $T_{wmin} = 790°C$ (see Fig. 2). The conode of the onset of the wetting phase transition for high-angle grain boundaries at $T_{wmin} = 790°C$ is shown in the bulk phase diagram (see Fig. 2). At this temperature, the grain boundaries with the maximum energy become completely wetted (see the scheme in Fig. 1).

A microstructure similar to that shown in Fig. 3a is formed immediately after the sample is heated to the eutectic temperature $T_e = 780°C$. Before the heating of the sample, the silver particles are uniformly distributed in the fine-grained copper matrix. When the sample is heated to the eutectic temperature, the melt is formed, grains grow rapidly, and the moving grain boundaries "sweep" small particles of the silver-rich phase. As a result, such particles remain only at the center of grown grains (see Figs. 3a–3c and 4a), and the melt is almost completely collected at the grain boundaries and triple joints. Metal crystals grown from the melt always contain the so-called block structure, i.e., the network of low-angle dislocation boundaries. For copper bicrystals grown by the Bridgeman method, the misorientation angle of the blocks measured using electron backscattering diffraction (EBSD) method is approximately 0.8° [13]. Under our conditions (the melt is poured out in a vacuum to a cylindrical mold), copper grains grow 5–10 times faster than in the case of the growth of bicrystals; for this reason, their perfection is lower and the misorientation of the low-angle dispersion boundaries can be estimated as approximately 3°–5°.

Figure 3b shows the microstructure of the copper alloy with 10 wt % Ag after the annealing at a temperature of 900°C. Almost all high-angle grain boundaries in this structure are completely wetted. The last high-angle grain boundaries incompletely wetted by the melt disappear at $T_{wmax} = 1020°C$ (see Fig. 2). The conode of the finish of the wetting phase transition for high-angle grain boundaries at $T_{wmax} = 1020°C$ is shown in the bulk phase diagram (see Fig. 2). At this temperature, the grain boundaries with the minimum energy become completely wetted (see Fig. 1).

Figure 3c shows the microstructure of the copper alloy with 10 wt % Ag after the annealing at a temperature of 910°C. It is very similar to the microstructure shown in Fig. 3b. The fraction of the completely wetted high-angle grain boundaries in this case is larger than that in Fig. 3a, but is smaller than that in Fig. 3b. It is seen in Fig. 3b that, in addition to the completely wetted high-angle grain boundaries, a "web" of thin liquid layers penetrating from the high-angle grain boundaries filled with the melt inside the bulk of crystallites through the low-angle grain boundaries of the blocks (shown by the arrow) appears at some places. Such a
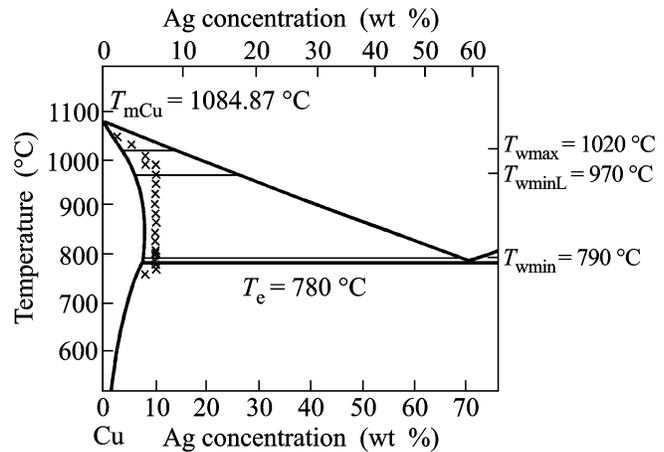
Fig. 2. Cu–Ag phase diagram. The thick lines indicate the volume phase transitions. The thin horizontal conodes are the lines of the onset and finish of the complete wetting for the high-angle and low-angle grain boundaries. The crosses mark the annealing temperatures and the compositions of the alloys under investigation.

web is absent in Fig. 3c. Figure 3d shows the copper sample with 10 wt % Ag after annealing at a higher temperature of 1010°C. It is clearly seen that the area covered by the web of thin liquid layers increases with the temperature. This indicates the active beginning of the wetting of low-angle grain boundaries of the blocks. The size of these blocks is about 50 μm. Thus, the onset temperature of the wetting of the block boundaries, $T_{wminL} = 970°C$, is somewhat lower than the finish temperature of the wetting transition for the high-angle grain boundaries, $T_{wmax} = 1020°C$ (see the corresponding conode in Fig. 2).

Figures 4a and 4b show the melt drops at the center of the grains far from the high-angle grain boundaries. At a temperature of 800°C (i.e., below T_{wminL}), these drops are round; their shape is close to spherical (see Figs. 3c and 4a). At a temperature of 1010°C (i.e., above T_{wminL}), these drops lose the round shape and are also transformed to the characteristic web of liquid layers along the block boundaries (see Fig. 4b). It is clearly seen in Fig. 4b that the liquid phase begins to penetrate to the block boundaries from the grain boundaries; i.e., the contact angle θ at the place where the low-angle block boundaries reach the interface between the solid and liquid phases above T_{wminL} is zero.

Below T_{wminL}, the contact angle θ at the place where the low-angle block boundaries reach the interface between the solid and liquid phases is nonzero. Far from T_{wminL} (see the structure shown in Fig. 4c for 870°C), it is nearly 180°; the melt layers at the high-angle grain boundaries are absolutely flat. The contact angle decreases continuously with an increase in temperature and its approach to T_{wminL}. In particular, the melt layers at high-angle grain boundaries at 950° (see
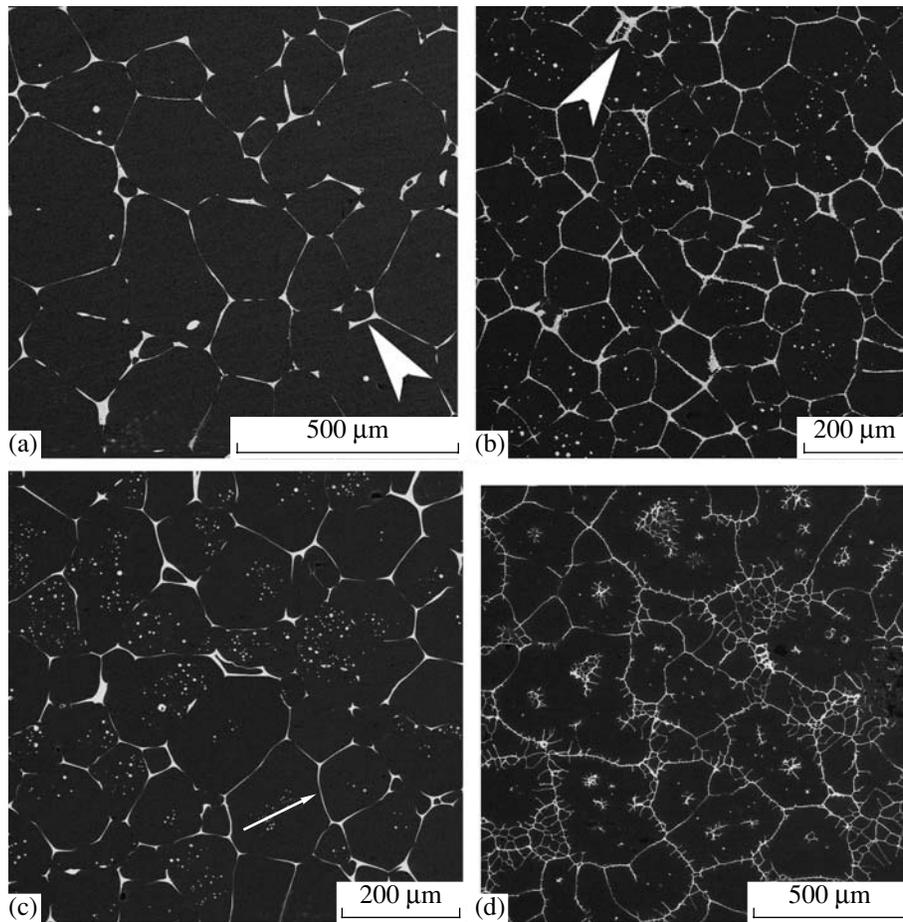
Fig. 3. Microstructures of the copper alloy with 10 wt % Ag after annealing in the two-phase region of the phase diagram (see Fig. 2) for (a) 800°C; in this case, the complete wetting of all high-angle grain boundaries is absent, the arrow shows one of the completely wetted grain boundaries; (b) 970°C; in this case, almost all high-angle grain boundaries are completely wetted and the first wetted low-angle grain boundaries appear (shown by the arrow); (c) 910°C; in this case, the fraction of completely wetted high-angle grain boundaries (one of which is marked by the arrow) is larger than that in panel (a), but is smaller than that in panel (b); and (d) 1010°C; in this case, the penetration of the liquid phase through the low-angle grain boundary is clearly seen.

Fig. 4d) form a comb of benches at the joints with the low-angle grain boundaries. In this case, the contact angle is approximately 90°. It decreases from 180° to zero in a narrow temperature range from 890 to 970°C. Belousov [11] pointed out that, in the case of the complete wetting of the entire low-angle grain boundary by the melt, the crystallites (grains) composing the material can be decomposed into small fragments with the formation of the lyophilic colloid solution.

The value $\sigma_{GB\,max} = 0.5 \pm 0.08$ J/m^2 measured using the zero creep method [14] can be used as an estimate of the maximum energy of high-angle grain boundaries (see scheme in Fig. 1). The minimum energy $\sigma_{GB\,min}$ in Fig. 1 corresponds to twin high-angle grain boundaries. The value $\sigma_{GB\,min} = 0.018 \pm 0.005$ J/m^2 [15] obtained in the measurement of dihedral angles at the point where the twin boundaries reach the outer surface can be used as an estimate of $\sigma_{GB\,min}$. The $\sigma_{GB\,min}$ value can also be estimated as the energy of a stacking fault in copper,

which was measured from the width of the equilibrium splitting of edge dislocations, $\sigma_{SF} = 0.04 \pm 0.005$ J/m^2 [16, 17]. Thus, $\sigma_{GB\,min} = 0.02$–0.04 J/m^2. Knowing that the coalescence of the liquid nuclei of dislocations begins at the misorientation angle $\theta_{w2} = 1.07b/R_F$ [9] and using modified expression (3) for the Frank radius R_F, one can estimate the energy of the interface between the liquid and solid phases at the temperature of the transition from the incomplete wetting of the low-angle grain boundaries to the complete wetting as

$$\sigma_{SL} = \theta_{w2}Gb/[8.56\pi^2(1-\nu)]. \qquad (4)$$

The substitution of $G = 48$ GPa, $\nu = 0.34$, and $b = 0.2556$ nm for copper [18] provides $\sigma_{SL} = 0.022$ J/m^2 for $\theta_{w2} = 0.1$ rad. From the complete wetting condition $\sigma_{GB} = 2\sigma_{SL}$, we obtain the value $\sigma_{GB\,maxL} = 0.044$ J/m^2, which is only slightly larger than the value $\sigma_{GB\,min} = 0.02$–0.04 J/m^2 (see Fig. 1). These energy estimates are
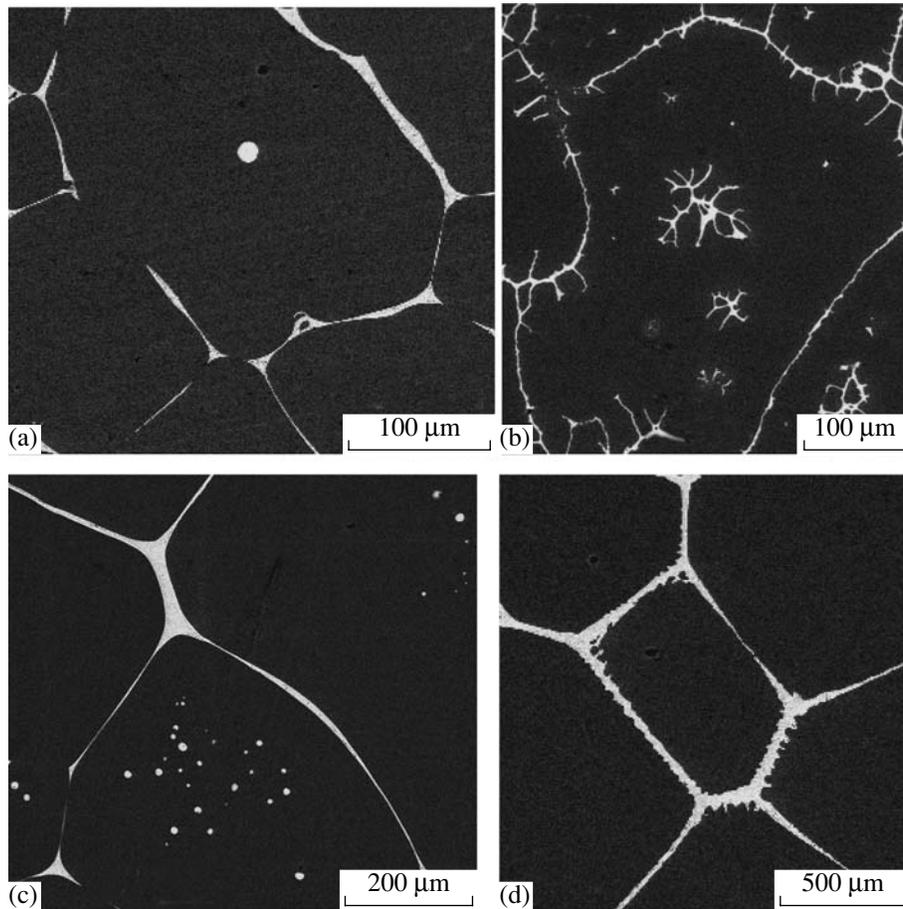
Fig. 4. Details of the microstructures of the copper alloy with 10 wt % Ag after annealing in the two-phase region of the phase diagram (see Figs. 2 and 3) for (a) 800°C; in this case, the liquid drops in the grain bulk have the round shape and do not wet the low-angle grain boundaries; (b) 1010°C; in this case, the liquid drops at the center of the grains wet the low-angle grain boundaries; (c) 870°C; in this case, the wetting layers at high-angle grain boundaries are smooth; and (d) 950°C; in this case, the wetting layers at high-angle grain boundaries are comb-like with benches at the joints with low-angle grain boundaries.

in agreement with the observed pattern when the transition to the complete wetting of the low-angle grain boundaries occurs at the temperature $T_{wminL} = 970$°C, which is much higher than the onset temperature of the complete wetting of the high-angle grain boundaries $T_{wmin} = 790$°C and is only slightly lower than the finish temperature of the wetting transition at high-angle grain boundaries, $T_{wmax} = 1020$°C.

Using the data from [9], one can show that, if $\sigma_{SL} = 0.022$ J/m^2 and the coalescence of the liquid nuclei of dislocations assumingly begins at the misorientation angle $\theta_{w2} = 1.07b/R_F = 0.1$ rad, the liquid nuclei of dislocations at the high-angle grain boundaries should be manifested at the critical misorientation angle $\theta_{w1} = 0.19b/R_F \approx 1$°.

Thus, as the temperature increases, the transition from the incomplete wetting of the low-angle grain boundaries to the complete wetting has been experimentally observed in this work. The complete wetting of high-angle grain boundaries in the copper–silver

alloys begins at the temperature $T_{wmin} = 790$°C, which is slightly higher than the eutectic reaction temperature $T_e = 780$°C. The onset temperature of the complete wetting of the low-angle grain boundaries in the copper–silver alloys, $T_{wminL} = 970$°C, is 50°C lower than the finish temperature of the wetting transition at the high-angle grain boundaries, $T_{wmax} = 1020$°C. The complete wetting of the low-angle grain boundaries occurs through the formation of thin (several microns) continuous layers of the liquid phase. The complete wetting of the low-angle grain boundaries through the formation of the liquid cylindrical channels at nuclei forming the low-angle grain boundaries of lattice dislocations is a problem for further experimental investigations.

REFERENCES

1. J. W. Cahn, J. Chem. Phys. **66**, 3667 (1977).
2. C. Ebner and W. F. Saam, Phys. Rev. Lett. **38**, 1486 (1977).
3. N. Eustathopoulos, Int. Met. Rev. **28**, 189 (1983).
4. B. B. Straumal, *Grain Boundary Phase Transitions* (Nauka, Moscow, 2003) [in Russian].
5. B. Straumal, T. Muschik, W. Gust, and B. Predel, Acta Metall. Mater. **40**, 939 (1992).
6. B. Straumal, D. Molodov, and W. Gust, J. Phase Equilibria **15**, 386 (1994).
7. A. P. Sutton and R. W. Balluffi, *Interfaces in Crystalline Materials* (Clarendon, Oxford, 1995).
8. J. P. Hirth and J. Lothe, *Theory of Dislocations* (McGraw Hill, New York, 1968).
9. E. Rabkin and I. Snapiro, Acta Mater. **48**, 4463 (2000).
10. F. C. Frank, Acta Crystall. **4**, 497 (1951).
11. V. V. Belousov, JETP Lett. **88**, 297 (2008).
12. L.-S. Chang, E. Rabkin, B. B. Straumal, et al., Acta Mater. **47**, 4041 (1999).
13. B. Straumal, S. Polyakov, E. Bischoff, and E. Mittemeijer, Zt. Metallkd. **95**, 939 (2004).
14. E. Gershman and S. Zhevnenko, Def. Diff. Forum **273–276**, 608 (2008).
15. R. L. Fullman, J. Appl. Phys. **22**, 448 (1951).
16. D. J. H. Cockaine, M. L. Jenkins, and I. L. F. Ray, Phil. Mag. **24**, 1383 (1971).
17. W. M. Stobbs and C. H. Sworn, Phil. Mag. **24**, 1365 (1971).
18. *Smithells Metals Reference Book*, 8th Ed. (Elsevier, Amsterdam, 2004).

Translated by R. Tyapaev